

Laser-induced breakdown by impact ionization in SiO₂ with pulse widths from 7 ns to 150 fs

D. Du, X. Liu, G. Korn, J. Squier, and G. Mourou
 Center for Ultrafast Optical Science, University of Michigan, Ann Arbor, Michigan 48109-2099

(Received 13 September 1993; accepted for publication 16 March 1994)

Results of laser-induced breakdown experiments in fused silica (SiO₂) employing 150 fs–7 ns, 780 nm laser pulses are reported. The avalanche ionization mechanism is found to dominate over the entire pulse-width range. Fluence breakdown threshold does not follow the scaling of $F_{th} \sim \sqrt{\tau_p}$, when pulses are shorter than 10 ps. The impact ionization coefficient of SiO₂ is measured up to $\sim 3 \times 10^8$ V/cm. The relative role of photoionization in breakdown for ultrashort pulses is discussed.

Laser-induced breakdown (LIB) in optically transparent materials has been studied extensively since the laser was invented in the 1960s.^{1–5} LIB mechanisms have been investigated for laser pulse widths down to tens of picoseconds. LIB remains an important topic because of its role in a wide range of high-power laser applications, where damage to optical components due to LIB often is the ultimate restriction on system performance. Increasingly, high laser power is achieved with moderate amount of energy (\sim joules) by reducing the pulse width from picoseconds to femtoseconds. Our present work is to investigate LIB in this important regime.

It is a well-established fact that the breakdown threshold depends on the pulse width of the laser pulses. An empirical scaling law of the fluence breakdown threshold for longer pulses ($\tau_p > 10$ ps) exists:⁶ $F_{th} \propto \sqrt{\tau_p}$. Until recently, the shortest pulses available for LIB studies were in the range of tens of picoseconds. However, new techniques in ultrashort laser pulse generation and amplification, such as the chirped-pulse amplification (CPA),⁷ have pushed the available pulse widths to the femtosecond regime. More importantly, CPA readily allows one to vary the laser pulse width continuously—up to hundreds of picoseconds—from a single laser system based on this principle. The setup of a LIB experiment using such a laser can therefore have a wide range of laser pulse widths, without changing other important parameters, such as the focusing of the pulse onto the sample.

We have performed a series of experiments to determine the LIB threshold as a function of laser pulse width between 150 fs and 7 ns, using a CPA laser system. The short-pulse laser used in our experiment was a 10-Hz Ti:sapphire oscillator-amplifier system based on the CPA technique. The laser pulse was focused by an $f=25$ cm lens inside the SiO₂ sample. The Rayleigh length of the focused beam is ~ 2 mm. The focused spot size was measured *in situ* by a microscope objective lens. The measured spot size (FWHM) was $26 \mu\text{m}$ in a Gaussian mode. The fused silica samples were made from Corning 7940, with a thickness of 0.15 mm. They were optically polished on both sides with a scratch/dig of 20-10. Each sample was cleaned by methanol before the experiment. Thin samples were used in order to avoid the complications of self-focusing of the laser pulses in the bulk. The SiO₂ sample was mounted on a computer-controlled motor-

ized X-Y translation stage. Each location on the sample was illuminated by the laser only once.

Two diagnostics were used to determine the breakdown threshold F_{th} . First, the plasma emission from the focal region was collected by a lens to a photomultiplier tube with appropriate filters. Second, the change of transmission through the sample was measured with an energy meter. Visual inspection was performed to confirm the breakdown at nanosecond pulse duration. Figure 1 shows typical plasma emission and transmitted light signal versus incident laser energy plots, at a laser pulse width of $\tau_p=300$ fs. It is worth noting that the transmission changed slowly at around F_{th} . This can be explained by the temporal and spatial behavior of the breakdown with ultrashort pulses. Due to the spatial variation of the intensity, the breakdown down reach threshold at the center of the focus, and because of the short pulse duration, the generated plasma will stay localized. The decrease in transmitted light is due to the reflection, scattering, and absorption by the plasma. By assuming a Gaussian profile in both time and space for the laser intensity, and further assuming that the avalanche takes the entire pulse duration to reach threshold, one can show that the transmitted laser energy U_t as a function of the input energy U is given by

$$U_t = \begin{cases} kU, & U \leq U_{th} \\ kU_{th}[1 + \ln(U/U_{th})], & U > U_{th} \end{cases} \quad (1)$$

where k is the linear transmission coefficient. The solid curve in Fig. 1 is plotted using Eq. (1), with U_{th} as a fitting

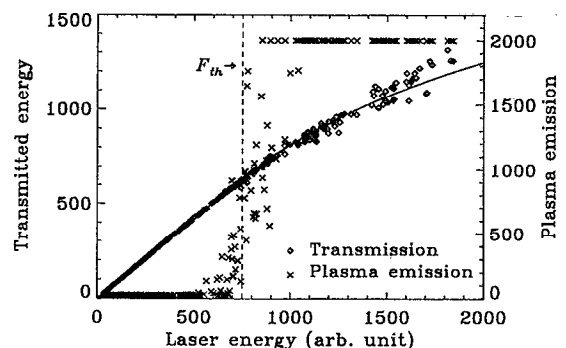


FIG. 1. Scattered plasma emission and transmitted laser pulse as a function of incident laser pulse energy.

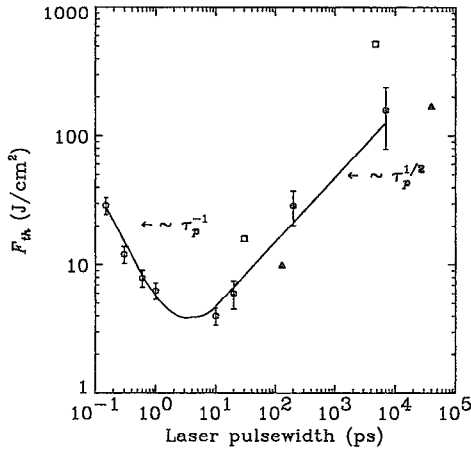


FIG. 2. Fluence threshold vs pulse width. The $\sqrt{\tau_p}$ scaling holds for pulse widths down to 10 ps, shown by the solid line. For longer pulse widths, previously obtained bulk (squares, see Ref. 4) and surface (triangles, Stokowski *et al.*, see Ref. 17) damage data are also shown.

parameter. In contrast, breakdown caused by nanosecond laser pulses cuts off the transmitted beam near the peak of the pulses,⁸ indicating a different temporal and spatial behavior.

Figure 2 shows the fluence breakdown threshold F_{th} as a function of laser pulse width. From 7 ns to about 10 ps, the breakdown threshold follows the scaling law of $F_{th} \propto \sqrt{\tau_p}$. Breakdown thresholds from earlier work in this pulse-width regime are also shown as a comparison—it can be seen that our data are consistent with earlier work. However, when the pulse width becomes shorter than a few picoseconds, the threshold starts to increase. This increase at shorter pulse widths may come as a surprise at first, but it still falls into the regime of an avalanche dominated process at high field strength, as we will show below.

The ionization process of a solid illuminated by an intense laser pulse can be described by the general equation³

$$\frac{dn_e(t)}{dt} = \eta(E)n_e(t) + \left(\frac{dn_e(t)}{dt}\right)_{PI} - \left(\frac{dn_e(t)}{dt}\right)_{loss}, \quad (2)$$

where $n_e(t)$ is the free electron (plasma) density, $\eta(E)$ is the avalanche coefficient, and E is the electric field strength. The second term on the right-hand side is the photoionization contribution, and the third term is the loss due to electron diffusion, recombination, etc. When the pulse width is in the picosecond regime, the loss of the electron is negligible during the duration of the short pulse.

Photoionization contribution can be estimated by the tunneling rate.⁹ For short pulses, $E \sim 10^8$ V/cm, the tunneling rate is estimated to be $w \sim 4 \times 10^9$ s⁻¹, which is small compared to that of avalanche, which is derived below. However, photoionization can provide the initial electrons needed for the avalanche processes at short pulse widths. For example, our data show at 1 ps, the rms field threshold is about 5×10^7 V/cm. The field will reach a value of 3.5×10^7 V/cm (rms) at 0.5 ps before the peak of the pulse, and $w \sim 100$ s⁻¹. During a $\Delta t \sim 100$ fs period the electron density can reach $n_e \sim n_i [1 - \exp(-w\Delta t)] \sim 10^{11}$ cm⁻³, where $n_i \sim 10^{22}$ is the total initial valence band electron density.

Neglecting the last two terms in Eq. (2), we then have the case of an electron avalanche process, with impact ionization by primary driven by the laser field. The electron density is then given by $n_e(t) = n_0 \exp[\eta(E)t]$, where n_0 is the initial free electron density. These initial electrons may be generated through thermal ionization of shallow traps or photoionization. When assisted by photoionization at short pulse regime, the breakdown is more deterministic, contrary to that of nanosecond pulses, where the breakdown is more statistical.¹⁰ According to the commonly accepted condition that breakdown occurs when the electron density exceeds $n_{th} \approx 10^{18}$ cm⁻³ and an initial density of $n_0 \approx 10^{10}$ cm⁻³, the breakdown condition is then given by $\eta\tau_p = 18$.^{2,10} For our experiment, it is more appropriate to use $n_{th} \approx 1.6 \times 10^{21}$ cm⁻³, the plasma critical density, hence the threshold is reached when $\eta\tau_p \approx 30$. There is some arbitrariness in the definition of plasma density relating to the breakdown threshold. However, the particular choice of plasma density does not change the dependence of threshold as function of pulse duration (the scaling law).

In our experiment, the applied electric field is on the order of a few tens of MV/cm and higher. Under such a high field, the electrons have an average energy of ~ 5 eV, and the electron collision time τ is less than 0.4 fs for electrons with energy $U \geq 5-6$ eV.¹¹ Electrons will make more than one collision during one period of the electric oscillation. Hence the electric field is essentially a dc field to those high energy electrons. The breakdown field at optical frequencies has been shown to correspond to dc breakdown field by the relationship³ $E_{th}^{rms}(\omega) = E_{th}^{dc}(1 + \omega^2\tau^2)^{1/2}$, where ω is the optical frequency and τ is the collision time.

In dc breakdown, the ionization rate per unit length, α , is used to describe the avalanche process, with $\eta = \alpha(E)v_{drift}$, where v_{drift} is the drift velocity of electrons. When the electric field is as high as a few MV/cm, the drift velocity of free electrons is saturated and independent of the laser electric field, $v_{drift} \approx 2 \times 10^7$ cm/s.¹²

Thorner¹³ has derived an expression for $\alpha(E)$ which is applicable for all electric field strengths, which is essential when comparing to our experimental data. The ionization rate per unit length of an electron is just eE/U_i times the probability, $P(E)$, that the electron has an energy $\geq U_i$, or $\alpha(E) = (eE/U_i)P(E)$. We denote E_{kT} , E_p , and E_i as threshold fields for electrons to overcome the decelerating effects of thermal, phonon, and ionization scattering, respectively. When the electric field is negligible, $E < E_{kT}$, so the distribution is essentially thermal, $P(E)$ is simply $\exp(-U_i/kT)$. Shockley¹⁴ showed $P(E) \sim \exp(-const/E)$ for $E_{kT} < E < E_p$. Wolff¹⁵ found $P(E) \sim \exp(-const/E^2)$ at higher fields ($E > E_p$). Thorner combined the three cases and gave an expression that satisfies both low and high field limits

$$\alpha(E) = \frac{eE}{U_i} \exp\left(-\frac{E_i}{E(1 + E/E_p) + E_{kT}}\right). \quad (3)$$

This leads to $F_{th} \propto E^2\tau_p \sim 1/\tau_p$, i.e., the fluence threshold will increase for ultrashort laser pulses when $E > \sqrt{E_p E_i}$ is satisfied.

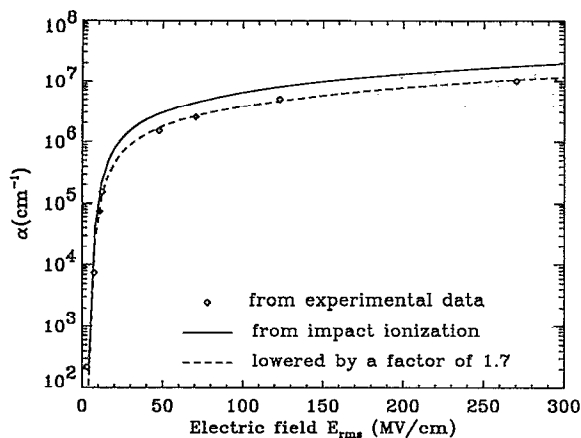


FIG. 3. Impact ionization rate per unit distance α determined from experiment and theory.

In Fig. 3, we plot α as a function of the electric field, E . From our experimental data, we calculate α according to $\eta\tau_p=30$ and $\eta=\alpha v_{\text{drift}}$. The solid curve is calculated from Eq. (3), using $E_i=30$ MV/cm, $E_p=3.2$ MV/cm, and $E_{kT}=0.01$ MV/cm. These parameters are calculated from $U=eEl$, where U is the appropriate thermal, phonon, and ionization energy, and l is the corresponding energy relaxation length ($l_{kT}=l_p\sim 5$ Å, the atomic spacing, and $l_i\approx 30$ Å, see Ref. 16 and the references therein). It shows the same saturation as the experimental data. The dashed line is corrected by a factor of 1.7, which results in an excellent fit with the experimental data. This factor of 1.7 is of relatively minor importance, as it can be due to a systematic correction, or because breakdown occurred on the surface first, which could have a lower threshold. The uncertainty of the saturation value of v_{drift} also can be a factor. The most important aspect is that the shape (slope) of the curve given by Eq. (3) provides excellent agreement with the experimental data. This prompts us to conclude that in our experiments, the mechanism of laser-induced breakdown in fused silica, using pulses as short as 150 fs and wavelength at 780 nm, is still dominated by the avalanche process.

In summary, we have investigated the pulse-width de-

pendence of the laser-induced optical breakdown threshold in fused silica with laser pulse widths over approximately five orders of magnitude, from 7 ns to 150 fs. We are able to obtain very good agreement, over the entire pulse-width range, on the ionization rate α between experiment and impact ionization theory. For picosecond pulses, evidence shows that photoionization is responsible for the initial electron generation. The plasma generated during breakdown with ultrashort pulses remains localized at the threshold, which could provide precise control of the interaction region for material processing and medical laser applications when ultrashort pulses are used. Our study is also relevant to solid-state microelectronics, as the structures become smaller and faster, electron transport properties under high fields and short durations—conditions explored in our experiment—will be increasingly important.

This work was funded by the Office of Naval Research and the National Science Foundation through the Center for Ultrafast Optical Science under STC PHY 8920108. We wish to thank T. Norris for helpful comments and P. Schermerhorn of Corning, Inc., who provided fused silica samples for the experiment.

- ¹ See the series of Proceedings of the Boulder Damage Symposium: Laser Induced Damage in Optical Materials (1969–92), Vols. 1–24.
- ² E. Yablonovitch and N. Bloembergen, *Phys. Rev. Lett.* **29**, 907 (1972).
- ³ N. Bloembergen, *IEEE J. Quantum Electron.* **QE-10**, 375 (1974).
- ⁴ W. L. Smith, *Opt. Eng.* **17**, 489 (1978).
- ⁵ S. C. Jones, P. Braunlich, R. T. Casper, X. -A. Shen, and P. Kelly, *Opt. Eng.* **28**, 1039 (1989).
- ⁶ J. R. Bettis, R. A. House II, and A. H. Guenther, in *Laser Induced Damage in Optical Materials: 1976*, NBS Spec. Pub. 462 (US GPO, Washington, DC, 1976), pp. 338–345.
- ⁷ D. Strickland and G. Mourou, *Opt. Commun.* **56**, 219 (1985).
- ⁸ D. W. Fradin, E. Yablonovitch, and M. Bass, *Appl. Opt.* **29**, 700 (1973).
- ⁹ M. V. Ammosov, N. B. Delone, and V. P. Krainov, *Sov. Phys. JETP* **64**, 1191 (1986).
- ¹⁰ D. Milam, Ref. 6, pp. 350–356.
- ¹¹ M. V. Fischetti and D. J. DiMaria, *Solid-State Electron.* **31**, 629 (1988).
- ¹² R. C. Hughes, *Solid-State Electron.* **21**, 251 (1978).
- ¹³ K. K. Thornber, *J. Appl. Phys.* **52**, 279 (1981).
- ¹⁴ W. Shockley, *Czech. J. Phys. B* **11**, 81 (1961).
- ¹⁵ P. A. Wolff, *Phys. Rev.* **95**, 1415 (1945).
- ¹⁶ D. J. DiMaria and J. R. Abernathy, *J. Appl. Phys.* **60**, 1727 (1986).
- ¹⁷ S. Stokowski, D. Milam, and M. Weber, in *Laser Induced Damage in Optical Materials: 1978*, NBS Spec. Pub. 541 (US GPO, Washington, DC, 1978), pp. 99–108.